Dublin Institute of Technology
ARROW@DIT

Articles | School of Electrical and Electronic Engineering

2006-08-01

Modeling Liquid-Crystal Devices with the Three-Dimensional Full-Vector Beam Propagation Method

Qian Wang
Dublin Institute of Technology

Gerald Farrell
Dublin Institute of Technology, gerald.farrell@dit.ie

Yuliya Semenova
Dublin Institute of Technology, yuliya.semenova@dit.ie

Follow this and additional works at: http://arrow.dit.ie/engscheceart

Part of the Electrical and Computer Engineering Commons

Recommended Citation

Wang, Q., Farrell, G., Semenova, Y.:Modeling Liquid-Crystal Devices with the Three-Dimensional Full-Vector Beam Propagation Method. Journal of the Optical Society of America A, Vol. 23 (8), 2006, pp.2014-2019.

This Article is brought to you for free and open access by the School of Electrical and Electronic Engineering at ARROW@DIT. It has been accepted for inclusion in Articles by an authorized administrator of ARROW@DIT. For more information, please contact yvonne.desmond@dit.ie, arrow.admin@dit.ie.

This work is licensed under a Creative Commons Attribution-Noncommercial-Share Alike 3.0 License

Modeling liquid-crystal devices with the three-dimensional full-vector beam propagation method

Qian Wang, Gerald Farrell, and Yuliya Semenova

Applied Optoelectronics Center, School of Electronics and Communications Engineering, Dublin Institute of Technology, Kevin Street, Dublin 8, Ireland

Received August 12, 2005; revised December 7, 2005; accepted March 7, 2006; posted March 16, 2006 (Doc. ID 64070)

Simulation of light propagation within nematic liquid-crystal (LC) devices is considered, of which the director is aligned normal to the z axis. A three-dimensional full-vector finite-difference beam propagation method for an anisotropic medium is presented and an alternating direction implicit scheme is adopted. Simulations of light propagation in a bulk polarization converter, a waveguide with a LC covering layer, and an integrated polarization splitter and optical switch are presented. Comparison with an existing simulation method is carried out for beam behavior within the bulk polarization converter. The effect of strong surface anchoring of a LC cell on the beam behaviors within the integrated switch is also demonstrated. © 2006 Optical Society of America

OCIS codes: 160.3710, 130.2790, 000.4430.

1. INTRODUCTION

Liquid-crystal- (LC-) based optical devices have been widely used in photonic information processing for its birefringence and electro-optical characteristics. Numerous application examples involve bulk LC displays, LC optical switches, and LC variable optical attenuators and polarization controllers.[1–4] LCs are also combined with photonic integrated circuits or photonic crystal circuits to construct, e.g., integrated optical switches, polarization splitters, or modulators that have a compact size and benefit from integration with a low fabrication cost.[5–9]

Accurate modeling and simulation of light behaviors are essential in developing these LC-based optical devices. For bulk LC devices, matrix methods, such as the Jones matrix method or the Berreman matrix method, are popularly used for their simplicity.[10,11] When the device structure is comparable to the scale of the wavelength, some numerical methods, such as the finite-difference (FD) time-domain method and the beam propagation method (BPM), have been employed based on a two-dimensional (2D) model of the device.[12–16] These simulation tools work well for some LC optical devices, such as LC gratings. However, for some other types of LC devices, such as LC-involved photonic integrated circuits, simulations based on a three-dimensional (3D) model are more desired since the channel waveguide has a finite cross section. However, most published investigations simulated the beam behaviors in integrated optical devices with the BPM based on a 2D approximation.[5,6] Therefore, in the present paper, a 3D FD BPM is presented in Section 2 for modeling and simulation of optical devices involving LCs, of which the director is aligned normal to the z axis. A full-vector BPM was presented in Ref. 16 for an anisotropic waveguide; however, it solved the BPM equations with sparse matrix solvers, such as ORTHORMIN or BICGSTAB. In the present paper, an alternating direction implicit (ADI) scheme is adopted, which simplifies the calculation procedure by its noniterative nature. Three numerical examples, namely, a bulk LC polarization converter, a waveguide with a LC covering layer, and an integrated optical switch and polarization splitter, are given in Section 3. Comparison with an existing simulation method is carried out for beam behavior within the bulk polarization converter. The effect of strong surface anchoring of the LC cell on the beam behaviors within the integrated switch is also demonstrated.

2. THREE-DIMENSIONAL FINITE-DIFFERENCE BEAM PROPAGATION METHOD WITH THE alternating DIRECTION IMPLICIT SCHEME

The full-vector wave equation of an electric field in a medium involving LCs is

$$\nabla \times \nabla \times \boldsymbol{E} - k^2 \hat{\epsilon} \boldsymbol{E} = 0, \tag{1}$$

where $k = 2\pi/\lambda_0$ and λ_0 is the wavelength in free space. $\hat{\epsilon}$ is the optical tensor of the LC and it has the following form when the director of LCs is aligned in the $x-y$ plane:

$$\hat{\epsilon} = \begin{bmatrix} \epsilon_{xx} & \epsilon_{xy} & 0 \\ \epsilon_{yx} & \epsilon_{yy} & 0 \\ 0 & 0 & \epsilon_{zz} \end{bmatrix} = \begin{bmatrix} n_o^2 + (n_e^2 - n_o^2)\cos^2\varphi & (n_e^2 - n_o^2)\cos\varphi\sin\varphi & 0 \\ (n_e^2 - n_o^2)\cos\varphi\sin\varphi & n_o^2 + (n_e^2 - n_o^2)\sin^2\varphi & 0 \\ 0 & 0 & n_o^2 \end{bmatrix}, \tag{2}$$

where n_o and n_e are ordinary and extraordinary refractive

 © 2006 Optical Society of America

indexes, respectively. φ is the angle between the x axis and the director. It could be the tilted angle or twisted angle of the director depending on the alignment of the LCs. With the approximation that $\partial\epsilon_{zz}/\partial_z \approx 0$, the wave equations for transverse components E_x and E_y are

$$\frac{\partial^2 E_x}{\partial y^2} + \frac{\partial^2 E_x}{\partial z^2} + k^2[\epsilon_{xx}E_x + \epsilon_{xy}E_y] = \frac{\partial^2 E_y}{\partial x\,\partial y} - \frac{\partial}{\partial x}\left[\frac{1}{\epsilon_{zz}}\frac{\partial}{\partial x}[\epsilon_{xx}E_x + \epsilon_{xy}E_y]\right] - \frac{\partial}{\partial x}\left[\frac{1}{\epsilon_{zz}}\frac{\partial}{\partial y}[\epsilon_{yx}E_x + \epsilon_{yy}E_y]\right], \tag{3a}$$

$$\frac{\partial^2 E_y}{\partial x^2} + \frac{\partial^2 E_y}{\partial z^2} + k^2[\epsilon_{yx}E_x + \epsilon_{yy}E_y] = \frac{\partial^2 E_x}{\partial x\,\partial y} - \frac{\partial}{\partial y}\left[\frac{1}{\epsilon_{zz}}\frac{\partial}{\partial x}[\epsilon_{xx}E_x + \epsilon_{xy}E_y]\right] - \frac{\partial}{\partial y}\left[\frac{1}{\epsilon_{zz}}\frac{\partial}{\partial y}[\epsilon_{yx}E_x + \epsilon_{yy}E_y]\right]. \tag{3b}$$

Assume that $E_i = \hat{E}_i \exp(jkn_0 z)$, $(i = x, y)$ (the slowly varying envelope approximation) and take the paraxial assumption, i.e., neglect the second-order derivative term of the envelope field on z. Equations (3a) and (3b) these become the full-vector paraxial beam propagation equations:

$$\frac{\partial}{\partial z}\left(\begin{bmatrix}\hat{E}_x\\ \hat{E}_y\end{bmatrix}\right) = \begin{bmatrix}P_{xx} & P_{xy}\\ P_{yx} & P_{yy}\end{bmatrix}\begin{bmatrix}\hat{E}_x\\ \hat{E}_y\end{bmatrix}, \tag{4}$$

where the operators P_{xx}, P_{xy}, P_{yx}, and P_{yy} are

$$P_{xx}\hat{E}_x = \frac{j}{2kn_0}\left\{\frac{\partial^2 \hat{E}_x}{\partial y^2} + \frac{\partial}{\partial x}\left[\frac{1}{\epsilon_{zz}}\frac{\partial}{\partial x}(\epsilon_{xx}\hat{E}_x)\right] + \frac{\partial}{\partial x}\left[\frac{1}{\epsilon_{zz}}\frac{\partial}{\partial y}(\epsilon_{yx}\hat{E}_x)\right] + k^2[(\epsilon_{xx} - n_0^2)\hat{E}_x]\right\}, \tag{5a}$$

$$P_{xy}\hat{E}_y = \frac{j}{2kn_0}\left\{k^2[\epsilon_{xy}\hat{E}_y] + \frac{\partial}{\partial x}\left[-\frac{\partial \hat{E}_y}{\partial y} + \frac{1}{\epsilon_{zz}}\frac{\partial}{\partial y}(\epsilon_{yy}\hat{E}_y) + \frac{1}{\epsilon_{zz}}\frac{\partial}{\partial x}(\epsilon_{xy}\hat{E}_y)\right]\right\}, \tag{5b}$$

$$P_{yx}\hat{E}_x = \frac{j}{2kn_0}\left\{k^2[\epsilon_{yx}\hat{E}_x] + \frac{\partial}{\partial y}\left[-\frac{\partial \hat{E}_x}{\partial x} + \frac{1}{\epsilon_{zz}}\frac{\partial}{\partial x}(\epsilon_{xx}\hat{E}_x) + \frac{1}{\epsilon_{zz}}\frac{\partial}{\partial y}(\epsilon_{yx}\hat{E}_x)\right]\right\}, \tag{5c}$$

$$P_{yy}\hat{E}_y = \frac{j}{2kn_0}\left\{\frac{\partial^2 \hat{E}_y}{\partial x^2} + \frac{\partial}{\partial y}\left[\frac{1}{\epsilon_{zz}}\frac{\partial}{\partial y}(\epsilon_{yy}\hat{E}_y)\right] + \frac{\partial}{\partial y}\left[\frac{1}{\epsilon_{zz}}\frac{\partial}{\partial x}(\epsilon_{xy}\hat{E}_y)\right] + k^2[(\epsilon_{yy} - n_0^2)\hat{E}_y]\right\}. \tag{5d}$$

To solve Eq. (4) noniteratively, an ADI scheme is adopted in the present paper, which was developed for full-vector BPM with isotropic dielectric structures.[17] First, by splitting the operators P_{xx} and P_{yy}, Eq. (4) can be written as

$$\frac{\partial}{\partial z}\left(\begin{bmatrix}\hat{E}_x\\ \hat{E}_y\end{bmatrix}\right) = \begin{bmatrix}P_{xx}^x + P_{xx}^y + C_{xy} & P_{xy}\\ P_{yx} & P_{yy}^x + P_{yy}^y + C_{yx}\end{bmatrix}\begin{bmatrix}\hat{E}_x\\ \hat{E}_y\end{bmatrix}, \tag{6}$$

where

$$P_{xx}^x\hat{E}_x = \frac{\partial}{\partial x}\left[\frac{1}{\epsilon_{zz}}\frac{\partial}{\partial x}(\epsilon_{xx}\hat{E}_x)\right] + \frac{k^2}{2}[(\epsilon_{xx} - n_0^2)\hat{E}_x],$$

$$P_{xx}^y\hat{E}_x = \frac{\partial^2 \hat{E}_x}{\partial y^2} + \frac{k^2}{2}[(\epsilon_{xx} - n_0^2)\hat{E}_x],$$

$$C_{xy}\hat{E}_x = \frac{\partial}{\partial x}\left[\frac{1}{\epsilon_{zz}}\frac{\partial}{\partial y}(\epsilon_{yx}\hat{E}_x)\right].$$

Similarly,

$$P_{yy}^x\hat{E}_y = \frac{\partial^2 \hat{E}_y}{\partial x^2} + \frac{k^2}{2}[(\epsilon_{yy} - n_0^2)\hat{E}_y],$$

$$P_{yy}^y\hat{E}_y = \frac{\partial}{\partial y}\left[\frac{1}{\epsilon_{zz}}\frac{\partial}{\partial y}(\epsilon_{yy}\hat{E}_t)\right] + \frac{k^2}{2}[(\epsilon_{yy} - n_0^2)\hat{E}_y],$$

$$C_{yx}\hat{E}_y = \frac{\partial}{\partial y}\left[\frac{1}{\epsilon_{zz}}\frac{\partial}{\partial x}(\epsilon_{xy}\hat{E}_y)\right].$$

For Eq. (6), with the Crank–Nicholson scheme, we have

$$\frac{1}{\Delta z}\left\{\begin{bmatrix}\hat{E}_x\\ \hat{E}_y\end{bmatrix}^{n+1} - \begin{bmatrix}\hat{E}_x\\ \hat{E}_y\end{bmatrix}^{n}\right\} = \frac{1}{2}\left\{\begin{bmatrix}P_{xx}^x & P_{xy}\\ 0 & P_{yy}^x\end{bmatrix} + \begin{bmatrix}P_{xx}^y & 0\\ P_{yx} & P_{yy}^y\end{bmatrix} + \begin{bmatrix}C_{xy} & 0\\ 0 & C_{yx}\end{bmatrix}\right\} \times \left\{\begin{bmatrix}\hat{E}_x\\ \hat{E}_y\end{bmatrix}^{n+1} - \begin{bmatrix}\hat{E}_x\\ \hat{E}_y\end{bmatrix}^{n}\right\}. \tag{7}$$

An approximation for $\frac{1}{2}\begin{bmatrix}C_{xy} & 0\\ 0 & C_{yx}\end{bmatrix}\left\{\begin{bmatrix}\hat{E}_x\\ \hat{E}_y\end{bmatrix}^{n+1} + \begin{bmatrix}\hat{E}_x\\ \hat{E}_y\end{bmatrix}^{n}\right\}$ is made for Eq. (7), i.e., $\begin{bmatrix}C_{xy} & 0\\ 0 & C_{yx}\end{bmatrix}\begin{bmatrix}\hat{E}_x\\ \hat{E}_y\end{bmatrix}^{n}$ is used instead. Therefore, Eq. (7) becomes

$$\frac{1}{\Delta z}\left\{\begin{bmatrix}\hat{E}_x\\ \hat{E}_y\end{bmatrix}^{n+1}-\begin{bmatrix}\hat{E}_x\\ \hat{E}_y\end{bmatrix}^{n}\right\}$$
$$=\frac{1}{2}\left\{\begin{bmatrix}P_{xx}^x & P_{xy}\\ 0 & P_{yy}^x\end{bmatrix}+\begin{bmatrix}P_{xx}^y & 0\\ P_{yx} & P_{yy}^y\end{bmatrix}\right\}\left\{\begin{bmatrix}\hat{E}_x\\ \hat{E}_y\end{bmatrix}^{n+1}+\begin{bmatrix}\hat{E}_x\\ \hat{E}_y\end{bmatrix}^{n}\right\}+\begin{bmatrix}C_{xy} & 0\\ 0 & C_{yx}\end{bmatrix}\begin{bmatrix}\hat{E}_x\\ \hat{E}_y\end{bmatrix}^{n}. \tag{8}$$

For Eq. (8), by adding high-order errors, it has the form

$$\begin{bmatrix}\hat{E}_x\\ \hat{E}_y\end{bmatrix}^{n+1}=\frac{\left(1+\frac{\Delta z}{2}\begin{bmatrix}P_{xx}^y & 0\\ P_{yx} & P_{yy}^y\end{bmatrix}\right)\left(1+\frac{\Delta z}{2}\begin{bmatrix}P_{xx}^x & P_{xy}\\ 0 & P_{yy}^x\end{bmatrix}\right)}{\left(1-\frac{\Delta z}{2}\begin{bmatrix}P_{xx}^y & 0\\ P_{yx} & P_{yy}^y\end{bmatrix}\right)\left(1+\frac{\Delta z}{2}\begin{bmatrix}P_{xx}^x & P_{xy}\\ 0 & P_{yy}^x\end{bmatrix}\right)}\times\begin{bmatrix}\hat{E}_x\\ \hat{E}_y\end{bmatrix}^{\bar{n}}, \tag{9}$$

where

$$\begin{bmatrix}\hat{E}_x\\ \hat{E}_y\end{bmatrix}^{\bar{n}}=\left(1+\Delta z\begin{bmatrix}C_{xy} & 0\\ 0 & C_{yx}\end{bmatrix}\right)\begin{bmatrix}\hat{E}_x\\ \hat{E}_y\end{bmatrix}^{n}.$$

Equation (9) can be easily solved by two steps. The equations for the first step are

$$\hat{E}_y^{n+(1/2)}-\frac{\Delta z}{2}P_{yy}^x\hat{E}_y^{n+(1/2)}=\hat{E}_y^{\bar{n}}+\frac{\Delta z}{2}P_{yy}^y\hat{E}_y^{\bar{n}}+\frac{\Delta z}{2}P_{yx}\hat{E}_x^{\bar{n}}, \tag{10a}$$

$$\hat{E}_x^{n+1/2}-\frac{\Delta z}{2}P_{xx}^xE_x^{n+(1/2)}=\hat{E}_x^{\bar{n}}+\frac{\Delta z}{2}P_{xx}^y\hat{E}_y^{\bar{n}}+\frac{\Delta z}{2}P_{xy}\hat{E}_y^{n+(1/2)}, \tag{10b}$$

and the equations for the second step are

$$\hat{E}_x^{n+1}-\frac{\Delta z}{2}P_{xx}^y\hat{E}_y^{n+1}=\hat{E}_x^{n+(1/2)}+\frac{\Delta z}{2}P_{xx}^xE_x^{n+(1/2)}+\frac{\Delta z}{2}P_{xy}\hat{E}_y^{n+(1/2)}, \tag{11a}$$

$$\hat{E}_y^{n+1}-\frac{\Delta z}{2}P_{yy}^y\hat{E}_y^{n+1}=\hat{E}_y^{n+(1/2)}+\frac{\Delta z}{2}P_{yy}^x\hat{E}_y^{n+(1/2)}+\frac{\Delta z}{2}P_{yx}\hat{E}_x^{n+1}. \tag{11b}$$

Obviously these equations are tridiagonal matrix equations, which are equivalent to 2D beam propagation problems. The transparent condition or perfectly matched layer can be used at the edges of the calculation region.[18,19]

With these BPM equations, modeling of beam behaviors within a bulk LC linear polarization converter, a waveguide with a LC covering layer, and an integrated LC switch and polarization splitter are now presented in Section 3.

3. NUMERICAL EXAMPLES

A. Bulk Liquid-Crystal Linear Polarization Converter

Both twisted and parallel-aligned LC cells with specific configurations can perform the function of linear polarization converting. Here a 90° twisted nematic LC cell is chosen to be a numerical example. The ordinary and extraordinary refractive indices of LCs are 1.5 and 1.7 at a wavelength of 1550 nm, respectively. According to analysis by the Jones matrix, it is known that when the cell thickness $d=(\sqrt{3}\lambda)/[2(n_e-n_o)]$, the input linear polarization direction can be ideally rotated by 90° when the light passes through LC cell. Suppose the rubbing direction of the first surface is along the x axis and for the second surface it is along the y axis. With the above full-vector FD BPM, the propagation of an E_x-polarized Gaussian beam with $\omega_0=10\ \mu$m within this LC cell is modeled and the corresponding results (power of the respective polarization component versus the propagation distance) are presented in Fig. 1. For comparison, the simulation results obtained with the Jones matrix are also presented in Fig. 1. One can see that these calculated results obtained by the above 3D full-vector FD BPM and Jones matrix are in good agreement.

In practical simulations, the items

$$\frac{\partial}{\partial x}\left[\frac{1}{\epsilon_{zz}}\frac{\partial}{\partial y}(\epsilon_{yx}E_x)\right],\quad \frac{\partial}{\partial y}\left[\frac{1}{\epsilon_{zz}}\frac{\partial}{\partial x}(\epsilon_{xy}E_y)\right],$$
$$\frac{\partial}{\partial x}\left[\frac{1}{\epsilon_{zz}}\frac{\partial}{\partial x}(\epsilon_{xy}E_y)\right],\quad \frac{\partial}{\partial y}\left[\frac{1}{\epsilon_{zz}}\frac{\partial}{\partial y}(\epsilon_{yx}E_x)\right]$$

in the above 3D full-vector FD BPM are small and can be neglected. Light propagation within this polarization converter is simulated by the FD BPM while neglecting these four items, and the corresponding results are presented in Fig. 1 as circles. One can see that they also have good agreement with the results obtained by the other two approaches.

B. Eigenmode of a Three-Dimensional Waveguide with a Liquid-Crystal Covering Layer

The eigenmode solution of a 3D waveguide with a LC covering layer is essential work for the modeling of integrated LC devices. In this numerical example, a channel

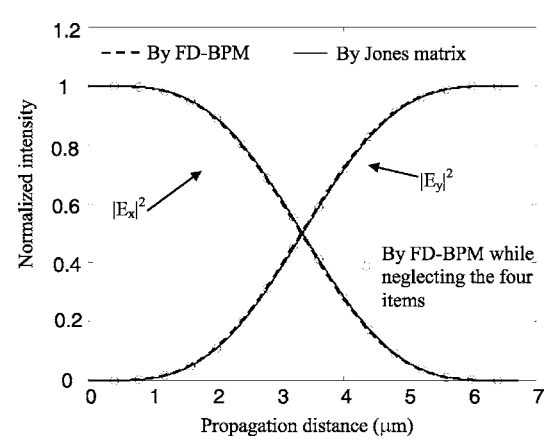

Fig. 1. Normalized power of the polarization component versus the propagation distance within a twisted nematic LC cell.

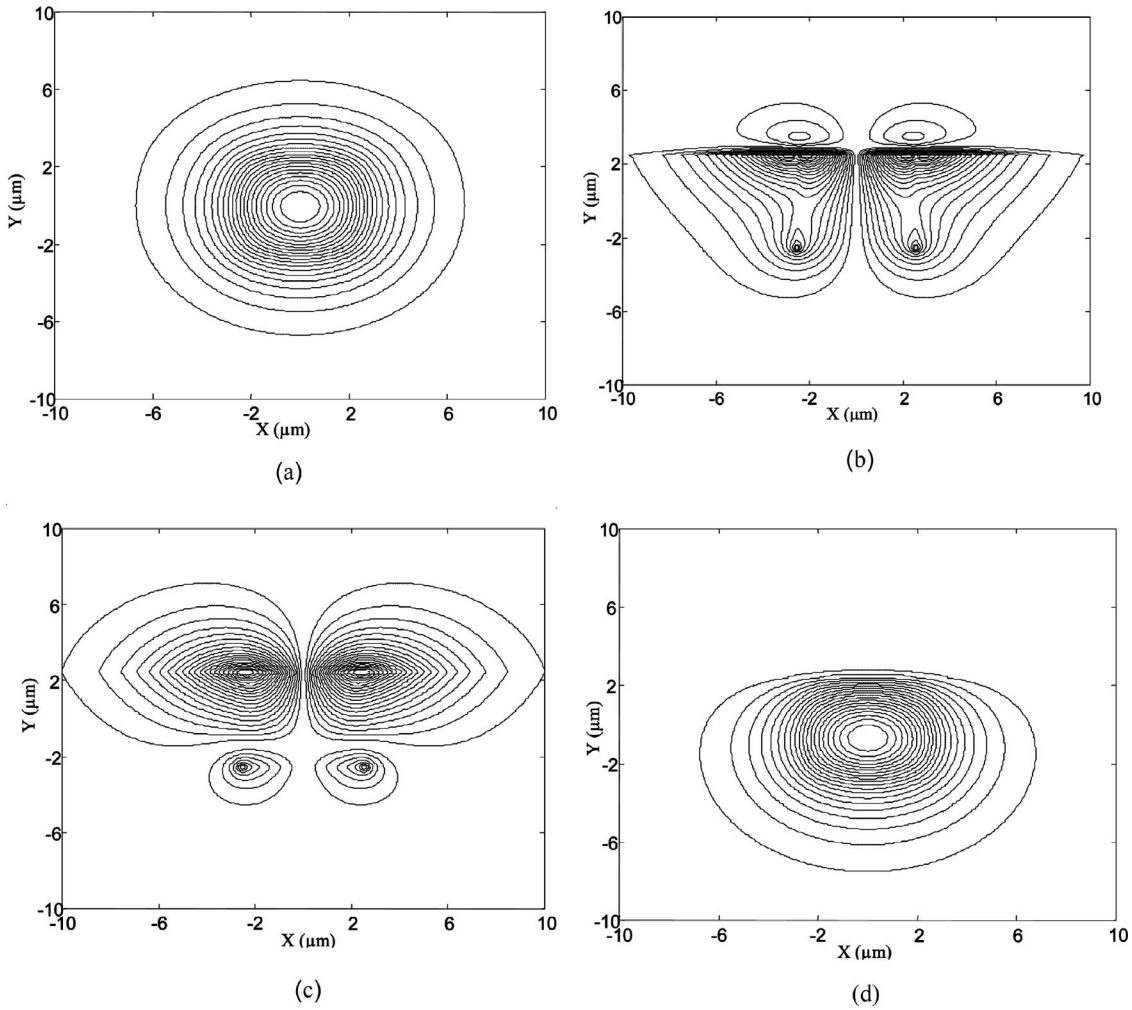

Fig. 2. Full-vector eigenmodes of a waveguide with a parallel-aligned LC covering layer: (a) E_x of the TE mode, (b) E_y of the TE mode, (c) E_x of the TM mode, (d) E_y of the TM mode.

waveguide of cross section 5 μm $\times$ 5 μm is considered. The LC used in the above example is chosen as the covering layer with parallel alignment. The refractive indices of the core and cladding of the waveguide are assumed to be 1.71 and 1.7, respectively. With the above-developed 3D full-vector BPM and the imaginary-distance BPM technique,[20] E_x and E_y components for the TE mode are presented in Figs. 2(a) and 2(b). Its effective refractive index is 1.70784. Correspondingly, field distributions of the TM mode are presented in Figs. 2(c) and 2(d). The effective index for the TM mode is 1.70670.

C. Integrated Polarization Splitter and Optical Switch

The third numerical example considered is an integrated polarization splitter and optical switch. Figure 3 presents the schematic configuration, which is a directional coupler containing a layer of LC (actually it is a LC cell with waveguides on both substrates). The same LC parameters and waveguide index profile are chosen as in the above. The separation of the two waveguides, i.e., the thickness of the LC layer, is 5 μm and the length of the directional coupler is 4000 μm. Light propagation in this device will be investigated based on the 3D model under three cases: (1) off state (no applied voltage); (2) high applied voltage (10 V), but strong surface anchoring; and (3) high applied voltage, but ideal weakly surface anchoring (all of the LC director ideally realigned parallel with the y axis). For these three cases, the eigenmodes of waveguide B calculated by the above example are chosen to be the input fields. With this full-vector 3D FD BPM, the propagation of the input fields along the directional coupler is calculated and the simulation results are shown in Figs. 4(a)–4(f) for these three cases. The normalized powers in

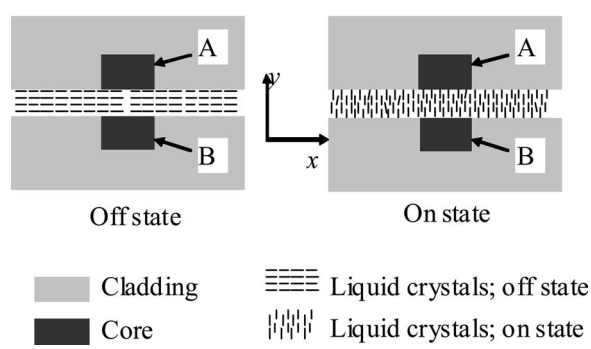

Fig. 3. Schematic configuration of an integrated polarization splitter and optical switch.

waveguide B for TE and TM modes along the propagation distance are presented in Fig. 5.

The calculation results for case one [Figs. 4(a) and 4(b) and the solid curves in Fig. 5] indicate that within the length of 4000 μm in this numerical example, light is coupled from waveguide B to waveguide A for the TE mode. However, for the TM mode, the light is well confined in waveguide B; in this case it can be used as a polarization splitter. It is known that the LC director will be realigned when there is an appropriate applied voltage. For the strong anchoring case, the director in the middle of the cell becomes almost parallel to the y axis, but at the LC cell surface, it still keeps the same alignment even when the applied voltage is high. In case two, the applied voltage is assumed to be 10 V and the exact profile of the LC director is solved by the iterative FD method proposed in Ref. 21. The parameters involved in solving the director profile are $k_{11}=11.7\times10^{-12}$ N, $k_{22}=9.0\times10^{-12}$ N, $k_{33}=19.5\times10^{-12}$ N, $\epsilon_{\parallel}=19.2$, $\epsilon_{\perp}=5.3$). Corresponding simulation results [Figs. 4(c) and 4(d), and dotted curves in Fig.

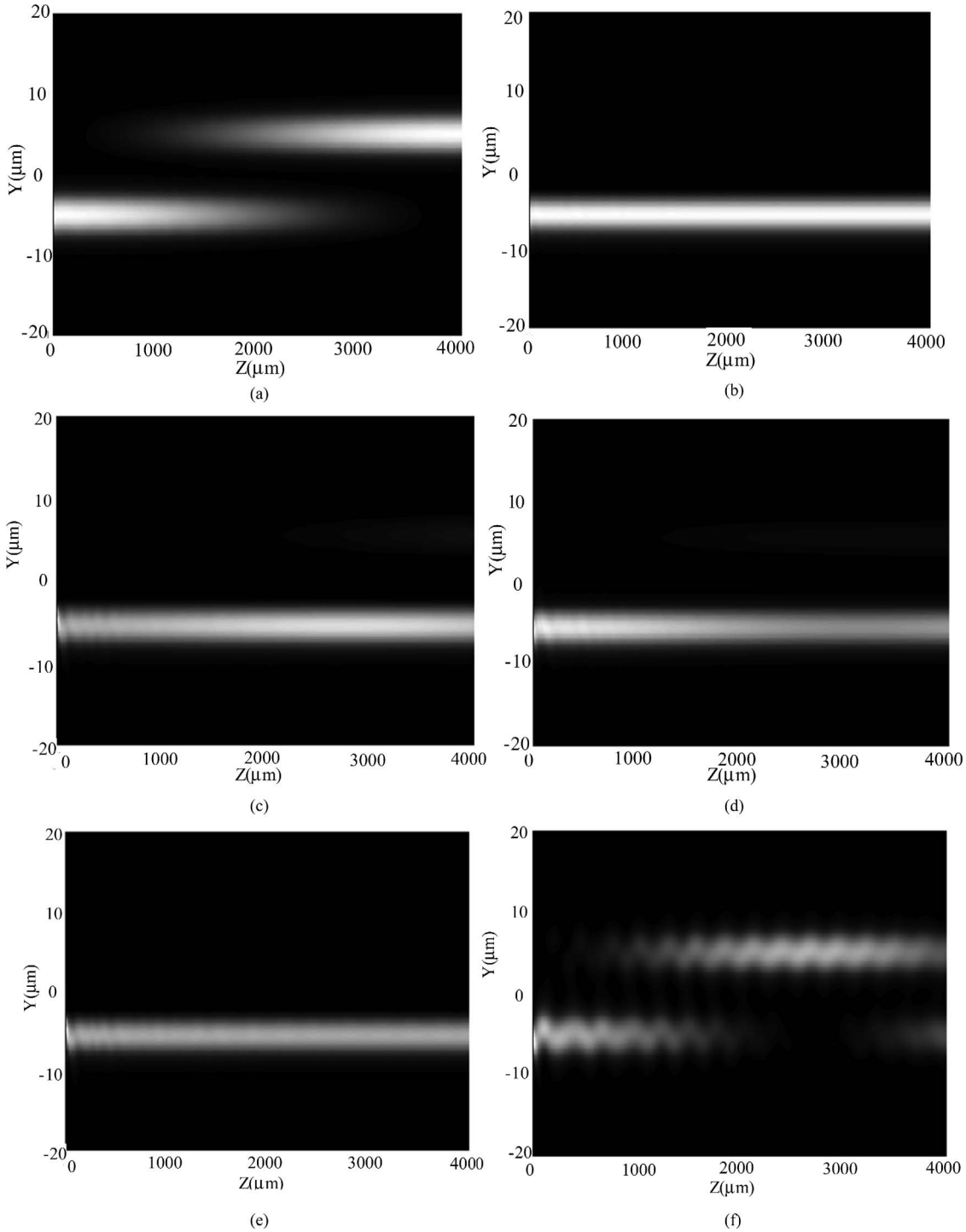

Fig. 4. Light propagation within the directional coupler for three cases: (a) TE mode and (b) TM mode for case one; (c) TE mode and (d) TM mode for case two; (e) TE mode and (f) TM mode for case three.

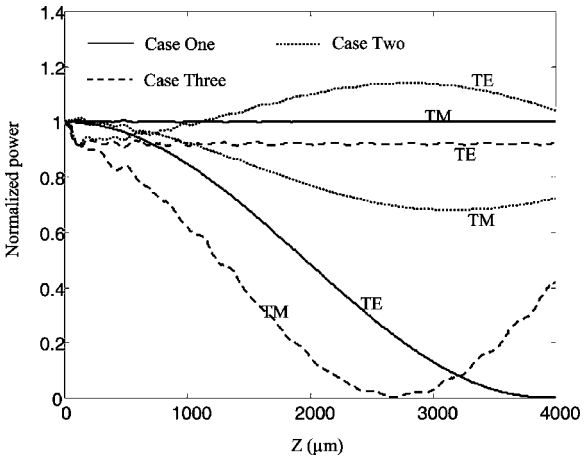

Fig. 5. Normalized power in waveguide B versus propagation distance for the three cases.

5] indicate that in this case, both TE and TM modes are basically confined in waveguide B and the TM mode is coupled to the TE mode while propagating along the device. For case three (the LC director is aligned vertically throughout the cell), the TM mode is coupled between waveguide A and B instead of remaining in waveguide B, as happened in the above two cases, and the TE mode is confined in waveguide B instead. The difference in simulation results between case two and case three shows that surface anchoring plays an important role in the device performance. The results in Fig. 5 also suggest that for this device to work as an optical switch, the coupling length should be $\sim 4000\,\mu$m for the TE mode and $\sim 2750\,\mu$m for the TM mode.

4. CONCLUSION

Light propagation within LC devices, of which the director is aligned normal to the light propagating direction, has been simulated. The three-dimensional full-vector finite-difference beam propagation method with an alternating direction implicit scheme for an anisotropic medium has been presented. Beam propagation within the bulk LC linear polarization converter has been modeled and the simulation results agree well with those obtained by the Jones matrix method. As numerical examples of an integrated LC device, the full-vector eigenmodes of a waveguide with an LC covering layer has been solved. Finally, the integrated polarization splitter/optical switch has been modeled and beam behaviors within this device have been simulated for both ON and OFF states. The effect of strong surface anchoring on the device performance has been demonstrated numerically.

The e-mail address for Q. Wang is qian.wang@dit.ie.

REFERENCES

1. N. A. Riza and S. Yuan, "Reconfigurable wavelength add–drop filtering based on a Banyan network topology and ferroelectric liquid crystal fiber-optic switches," J. Lightwave Technol. **17**, 1575–1584 (1999).
2. K. Wu, J. Liu, and Y. Chen, "Optical attenuator using polarization modulation and a feedback controller," U.S. patent 5,963,291 (5 October 1999).
3. K. Hirabayashi and C. Amano, "Liquid-crystal polarization controller arrays on planar waveguide circuits," IEEE Photon. Technol. Lett. **14**, 504–506 (2002).
4. Y. Semenova, Y. Panarin, G. Farrell, and S. Dovgalets, "Liquid crystal based optical switches," Mol. Cryst. Liq. Cryst. **413**, 2521–2534 (2004).
5. W. Y. Lee, J. S. Lin, and S. Y. Wang, "A novel vertical $\Delta\kappa$ directional coupler switch using liquid crystals," J. Lightwave Technol. **13**, 49–54 (1995).
6. K. C. Lin, W. C. Chuang, and W. Y. Lee, "Proposal and analysis of an ultrashort directional coupler polarization splitter with an NLC coupling layer," J. Lightwave Technol. **14**, 2517–2553 (1996).
7. D. B. Walker, E. N. Glytsis, and T. K. Gaylord, "Ferroelectric liquid-crystal waveguide modulation based on a switchable uniaxial–uniaxial interface" Appl. Opt. **35**, 3016–3030 (1996).
8. C. Y. Liu and L. W. Chen, "Tunable photonic-crystal waveguide Mach–Zehnder interferometer achieved by nematic liquid-crystal phase modulation," Opt. Express **12**, 2616–2624 (2004).
9. A. Fratalocchi, R. Asquini, and G. Assanto, "Integrated electro-optic switch in liquid crystals," Opt. Express **13**, 32–37 (2005).
10. P. Yeh and C. Gu, *Optics of Liquid Crystal Displays* (Wiley Interscience, 1999).
11. D. W. Berreman, "Optics in stratified and anisotropic media: 4×4 matrix formulation," J. Opt. Soc. Am. **62**, 505–510 (1972).
12. B. Witzigmann, P. Regli, and W. Fichtner, "Rigorous electromagnetic simulation of liquid crystals," J. Opt. Soc. Am. A **15**, 753–757 (1998).
13. E. E. Kriezis and S. J. Elston, "Finite-difference time domain method for light wave propagation within liquid crystal devices," Opt. Commun. **165**, 99–105 (1999).
14. E. E. Kriezis and S. J. Elston, "Light wave propagation in liquid crystal displays by the 2D finite-difference time-domain method," Opt. Commun. **177**, 69–77 (2000).
15. E. E. Kriezis and S. J. Elston, "Wide-angle beam propagation method for liquid-crystal device calculations," Appl. Opt. **39**, 5707–5714 (2000).
16. C. L. Xu, W. P. Huang, J. Chrostowski, and S. K. Chaudhuri, "A full-vector beam propagation method for anisotropic waveguides," J. Lightwave Technol. **12**, 1926–1931 (1994).
17. Y. L. Hsueh, M. C. Yang, and H. C. Chang, "Three-dimensional noniterative full-vectorial beam propagation method based on the alternating direction implicit method," J. Lightwave Technol. **17**, 2389–2397 (1999).
18. G. R. Hadley, "Transparent boundary condition for beam propagation," IEEE J. Quantum Electron. **28**, 363–370 (1992).
19. W. P. Huang, C. L. Xu, W. Lui, and K. Yokoyama, "The perfectly matched layer (PML) for the beam propagation method," IEEE Photon. Technol. Lett. **8**, 649–651 (1996).
20. S. Jungling and J. C. Chen, "A study and optimization of eigenmode calculations using the imaginary-distance beam-propagation method," IEEE J. Quantum Electron. **30**, 2098–2105 (1994).
21. Q. Wang, S. He, F. Yu, and N. Huang, "Iterative finite-difference method for calculating the distribution of a liquid-crystal director," Opt. Eng. **40**, 2552–2557 (2001).